

# We are IntechOpen, the world's leading publisher of Open Access books Built by scientists, for scientists

6,900

Open access books available

186,000

International authors and editors

200M

Downloads

Our authors are among the

154

Countries delivered to

TOP 1%

most cited scientists

12.2%

Contributors from top 500 universities



WEB OF SCIENCE™

Selection of our books indexed in the Book Citation Index  
in Web of Science™ Core Collection (BKCI)

Interested in publishing with us?  
Contact [book.department@intechopen.com](mailto:book.department@intechopen.com)

Numbers displayed above are based on latest data collected.  
For more information visit [www.intechopen.com](http://www.intechopen.com)



## Spiral Waves, Obstacles and Cardiac Arrhythmias

Daniel Olmos-Liceaga  
*University of Sonora*  
*México*

### 1. Introduction

The propagation of electrical waves through cardiac tissue is a very important phenomenon to study since those waves activate the mechanisms for cardiac contraction, responsible to pump blood to the body. An electrical wave of excitation, called also an action potential wave, is initiated periodically at a place called the sinoatrial node, the natural pacemaker of the heart. This wave, propagates throughout the atria where it arrives at the atrioventricular node, where after some time delay, it propagates to the ventricles via the Purkinje fibers (Zaret et al., 1992). In normal conditions, this process is repeated approximately 70 to 100 times each minute and is commonly referred to as a heartbeat. The condition at which abnormal generation or propagation of excitation waves during the process described above, is termed as arrhythmia.

One of the proposed mechanisms involved in the development of certain type of arrhythmias, are spiral waves, a particular form of functional reentry (Fenton et al., 2002; Veenhuyzen et al., 2004). Spiral waves, are self sustained waves of excitation that rotate freely or around an obstacle, reactivating the same area of tissue at a higher frequency than the normal SA node would do, increasing the normal heartbeat rate. In the worst scenario, a spiral wave might break up into smaller spiral waves giving uncoordinated contractions of the heart in a phenomenon known as fibrillation. When this phenomenon occurs in the ventricles, the heart quivers and loses its strength to pump blood to the body leading to immediate cardiac arrest (Fenton et al., 2002; Zaret et al., 1992). Fibrillation, is the main cause of death in industrialized countries (Fenton et al., 2002; Priori et al., 2002; Tang et al., 2005; Zipes, 2005).

An important research area is the study of the interaction of spiral waves in cardiac tissue with obstacles. Obstacles in cardiac tissue can be partially excitable or non excitable. Examples of partially excitable obstacles are scar tissue (Starobin et al., 1996) or ionic heterogeneities (Starobin et al., 1996; Tusscher & Panfilov, 2002; Valderrábano et al., 2000), whereas examples of non excitable obstacles are arteries (Valderrábano et al., 2000) or the natural orifices in the atria (Azene et al., 2001).

It has been observed that an obstacle in cardiac tissue might act as a stabilizer of spiral wave dynamics (Davidenko et al., 1992; Ikeda et al., 1997; Kim et al., 1999; Lim et al., 2006; Pertsov et al., 1993; Valderrábano et al., 2000), as it provides a transition between meandering spiral waves (Ikeda et al., 1997) or multiple spiral waves (Shajahan et al., 2007; Valderrábano et al., 2000) into a simple rotation spiral, which is attached to the obstacle. This

transition is clinically important because as it has been shown, fibrillation like activity changes to a tachycardia regime (Kim et al., 1999).

The interaction of spiral waves with obstacles and its relationship with the transition between different arrhythmic regimes has been experimentally and computationally studied by different researchers (Azene et al., 2001; Comtois & Vinet, 2005; Ikeda et al., 1997; Shajahan et al., 2007; 2009; Valderrábano et al., 2000). Valderrábano et al. (Valderrábano et al., 2000) studied in a cardiac tissue preparation the transition between ventricular fibrillation and ventricular tachycardia due to the presence of obstacles; Ikeda et al. (Ikeda et al., 1997), also considered the transition of different arrhythmic regimes due to the attachment of a spiral wave to an obstacle of minimum size. Shajahan et al. (Shajahan et al., 2007) used the Luo-Rudy and Panfilov models to study the transition of spiral turbulence to a simple rotating spiral wave due to the presence of an obstacle, which again provides a transition between different arrhythmic regimes; Xie et al. (Xie et al., 2001) presented a computational study of the effects of regional ischemia on the stability of a spiral wave; Azene et al. (Azene et al., 2001) carried out a computational study of the attachment and detachment of wavefronts to obstacles based on the Luo-Rudy model; Olmos (Olmos, 2010) studied the interaction of spiral waves in a particular case of the meandering regime, with rectangular obstacles. The aim in that work was to understand better necessary conditions in order to obtain attachment of the meandering spiral wave to the obstacle.

However, the interaction of spiral waves with obstacles and its relationship with transitions between different arrhythmic regimes, is a topic that has not been completely understood. For example, the interaction of a spiral wave in the meandering regime with an obstacle, has not previously been considered. Such interactions can be very complex (Olmos & Shizgal, 2008; Yermakova & Pertsov, 1986), and the determination of the conditions for which a meandering spiral wave attaches to an obstacle is an important endeavor. On the other hand, it has been considered that the presence of obstacles can be only of a stabilizing nature, which is not always the case. Therefore, the main objective of this work is to present a numerical study of the interaction of spiral waves with obstacles and to show the existence of different transitions due to the presence of obstacles.

By considering non-excitable and partially excitable obstacles we will show that obstacles cannot only stabilize the dynamics as shown in (Ikeda et al., 1997; Kim et al., 1999; Lim et al., 2006), but also, they can act as destabilizers. In both cases and by different mechanisms, the obstacle might act as a switch between two arrhythmic regimes, in which one is less dangerous than the other. In the case of non-excitable obstacles, it is shown that under certain conditions like the size of the obstacle, a more complex arrhythmia might appear.

To this end, this work will consist in the following sections. We start by presenting a general background about generation and propagation of action potentials (Section 2). In Section 3, we describe the model equations considered in the simulations. Then, in Section 4 the formation of a spiral wave is discussed. In the same section, we discuss the concepts of meandering and drift of spirals, which will be essential in explaining the results in this work. We follow this section by presenting the results obtained with partially excitable obstacles and non-excitable obstacles (Sections 5 and 6). We finish this work with Section 7 by presenting some conclusions, limitations and open questions in this topic.

## 2. Generation and propagation of an action potential

An important electrical property of atrial and ventricular cells is excitability. At rest, a ventricular cell has a transmembrane potential of about  $u = -84mV$  (Beeler & Reuter, 1977),

which is called the resting membrane potential (RMP). If a short time pulse of current is applied such that the new potential is below  $-60\text{mV}$ , the value of  $u$  will return to the RMP immediately. However, if the potential is raised above  $u = -60\text{mV}$ , the transmembrane potential will undergo a large excursion raising its value approximately to  $28\text{mV}$ , generating a peak, then a plateau and finally return to the RMP (Fig. 1). This phenomenon is called an action potential (AP) and cells with this property are called excitable cells. The value of  $u$  above which an AP is elicited, which in this case is  $u \approx -60\text{mV}$ , is called the threshold potential value  $u_{th}$ .

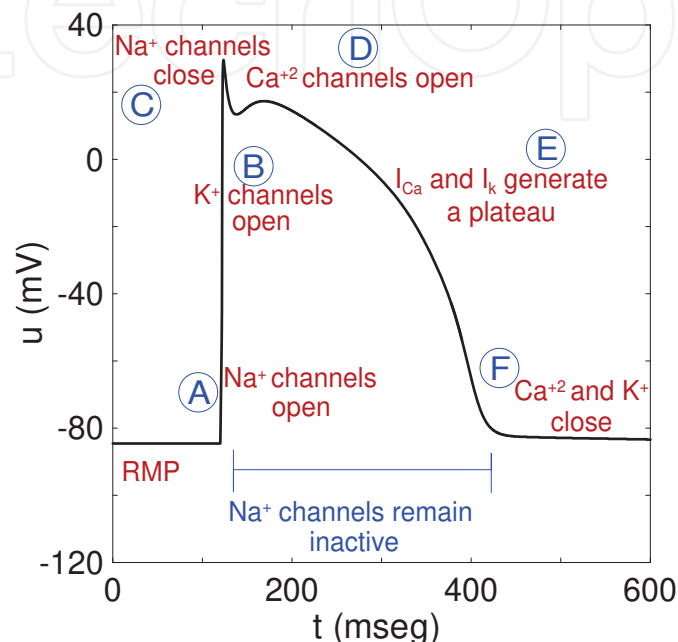


Fig. 1. Membrane potential  $u$  versus time during an AP. Representative mechanisms involved in the generation of an AP in a cardiac cell.

Changes in the membrane potential are due mainly to the passage of  $\text{Na}^+$ ,  $\text{K}^+$  and  $\text{Ca}^{++}$  ions via ion channels and other mechanisms through the cell membrane. The ion channels are membrane proteins which allow the passage across the membrane of specific type of ions between the interior and exterior of the cell. An essential part of the work by Hodgkin and Huxley (Hodgkin & Huxley, 1952) was to establish that the  $\text{Na}$ ,  $\text{K}$  and  $\text{Ca}$  channels can be opened or closed, and that state depends on the membrane potential at a given time.

The general mechanism by which an AP is generated is as follows: Initially the cell is at rest i.e. the potential across the cell membrane is at the RMP value. When the current is applied such that the new potential is above  $u_{th}$ ,  $\text{Na}$  channels open in a fast time scale and a flux of  $\text{Na}^+$  inside the cell, follows (Fig. 1A). The  $\text{Na}$  current is responsible for the rapid change in  $u$ , which changes dramatically from  $-60\text{mV}$  to  $28\text{mV}$  in a phenomenon called depolarization. In Fig. 1B,  $\text{K}$  channels open in a slow time scale compared to the time scale of the  $\text{Na}$  channels opening, and  $\text{K}^+$  flow outside the cell. In Fig. 1C, the  $\text{Na}$  channels close and the  $\text{K}^+$  current lowers the membrane potential generating a peak in the AP. After that,  $\text{Ca}$  channels open in a slow time scale and a flow of  $\text{Ca}^{++}$  from outside to inside the cell occurs (Fig. 1D). During this stage,  $\text{K}$  and  $\text{Ca}$  currents move in the opposite direction, generating what is called a plateau (Fig. 1E). Finally, both channels close and the membrane potential returns to the RMP value (Fig. 1F).

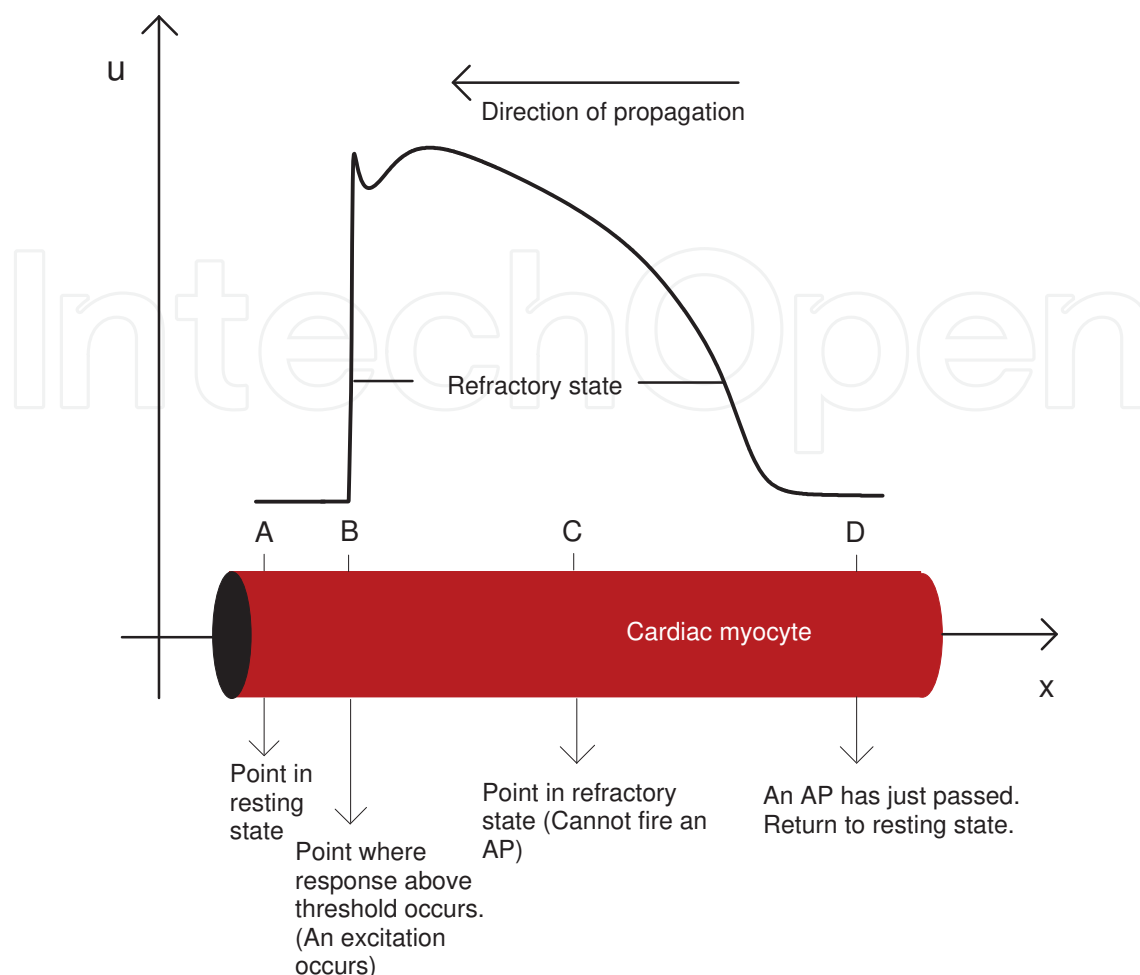


Fig. 2. Propagation of an AP. The propagation is taken over a hypothetical large myocyte.

Each location of the cell membrane, once it has a response above  $u_{th}$ , will experience an AP. The AP generated in a cell location, with the proper conditions (Kléber & Rudy, 2004), will propagate through the rest of the cell and through the cardiac tissue. The general mechanism by which an AP travels through cardiac muscle can be explained by considering a large single cell as shown in Fig. 2. In Fig. 2, it is considered that an AP is propagating only in the  $x$  direction and from right to left. At location A, the membrane potential is at the RMP value and it is ready to accept an AP. At point B, an AP has just been elicited. At point C, an AP is in process and at this location the cell is in refractory state and another AP cannot be generated. During this stage the  $Na$  channels, responsible for the depolarization of the cell, are closed and remain inactive for a time called the refractory period. Finally, at location D, an AP has just passed and at this location the membrane potential has almost returned to the RMP value. Therefore, the propagation of the AP is as follows. At location B, where the AP has just been elicited,  $Na$  ions are entering to the cell. These ions generate a current in the  $x$  direction due to the concentration gradient in a neighborhood of point B. These ions move to location A, increasing its corresponding  $u$  value until it reaches  $u_{th}$ . Then, an AP is elicited at location A and the AP advances in space. Therefore, propagation of the AP follows.

### 3. The model equations

In order to make simulations we consider equations of the reaction-diffusion type given by

$$\frac{\partial u}{\partial t} = \nabla \cdot (D \nabla u) - \frac{1}{C_m} (I_{ion}) \quad (1)$$

where,  $u$  is the transmembrane potential,  $D$  is the conductivity tensor,  $C_m$  is the capacitance and  $I_{ion}$  is the sum of the different ionic currents. There are different forms in which  $I_{ion}$  can be chosen, depending on which cell type is considered. For example the Luo-Rudy (Luo & Rudy, 1994) or the Priebe-Beuckelmann (Priebe & Beuckelmann, 1998) models are considered for ventricular cells, whereas the Courtemanche (Courtemanche et al., 1998) and the Nygren (Nygren et al., 1998) models were developed for atrial cells. Other models are the Yanagihara model for the sinoatrial node (Yanagihara et al., 1980), and the DiFrancesco-Noble model for the Purkinje cells (DiFrancesco & Noble, 1985). A complete list of models can be found in (Fenton & Cherry, 2008).

In this work, we consider the ionic currents given by Fenton and Karma (Fenton & Karma, 1998). This set of equations is a minimal model and was designed to mimic the behavior of complex models with a minimum number of variables. The Fenton-Karma (FK) equations are of the reaction diffusion type. They are given by

$$\begin{aligned} \frac{\partial u}{\partial t} &= \nabla \cdot (D \nabla u) - \frac{1}{C_m} (I_{fi} + I_{so} + I_{si}) \\ \frac{\partial v}{\partial t} &= \frac{1}{\tau_v} \Theta(u_c - u)(1 - v) - \frac{1}{\tau_v} \Theta(u_c - u)v \\ \frac{\partial w}{\partial t} &= \frac{1}{\tau_w} \Theta(u_c - u)(1 - w) - \frac{1}{\tau_w} \Theta(u_c - u)w \end{aligned} \quad (2)$$

where

$$\begin{aligned} I_{fi} &= -\frac{v}{\tau_d} \Theta(u - u_c)(1 - u)(u - u_c) \\ I_{so} &= \frac{u}{\tau_o} \Theta(u_c - u) + \frac{1}{\tau_r} \Theta(u - u_c) \\ I_{si} &= -\frac{w}{2\tau_{si}} (1 + \tanh[k(u - u_c^{si})]) \\ \tau_v^-(u) &= \Theta(u - u_v) \tau_{v1}^- + \Theta(u_v - u) \tau_{v2}^- \end{aligned} \quad (3)$$

In this case,  $u = u(x, t)$  measures the membrane potential at a location  $x$  and time  $t$ , whereas  $v$  and  $w$  are gate variables.  $I_{fi}$ ,  $I_{so}$  and  $I_{si}$  denote fast inward, slow outward and slow inward currents, respectively. Also  $D = 0.001$ ,  $C_m = 1$ ,  $\tau_d = 0.403$ ,  $\tau_r = 50.0$ ,  $\tau_{si} = 44.84$ ,  $\tau_o = 8.3$ ,  $\tau_v^+ = 3.33$ ,  $\tau_{v1}^- = 1000.0$ ,  $\tau_{v2}^- = 19.2$ ,  $\tau_w^+ = 667.0$ ,  $\tau_w^- = 11$ ,  $u_c = 0.13$ ,  $u_v = 0.055$ ,  $u_c^{si} = 0.85$ .  $\Theta(x)$  is the Heaviside step function. Numerically, we consider  $\Theta(x)$  as

$$\Theta(x) = \frac{1}{2}(1 + \tanh(50x))$$

Equations (2) are solved in a rectangular domain  $\Omega = [-7, 7] \times [-7, 7]$  using finite differences with  $N = 512$  points in each dimension. Advancing in time is done with Euler as in (Fenton & Karma, 1998) with  $dt = 0.125$ . At the domain boundary and at the boundary of non-excitable obstacles (Section 6), no-flux boundary conditions were imposed. Boundary conditions at obstacles were implemented as done in (Morton & Mayers, 2005).

### 4. Generation of a spiral wave

Spiral waves have been observed to occur in cardiac tissue (Ikeda et al., 1997; Isomura et al., 2008; Pertsov et al., 1993) and in computer models (Isomura et al., 2008; Olmos, 2010; Otani,

2000). There are different ways in which a spiral wave might be generated. For example, spiral waves arise when an unexcitable obstacle is stimulated with high frequency of AP (Panfilov & Kenner, 1993); they can also be generated by using the method of cross-field stimulation (Pertsov et al., 1993); and they might arise due to the appearance of ectopic beats (Otani, 2000). Ectopic beats can arise due to abnormal calcium cycling (Benson & Holden, 2005) or by overload of calcium inside the cell (Luo & Rudy, 1994).

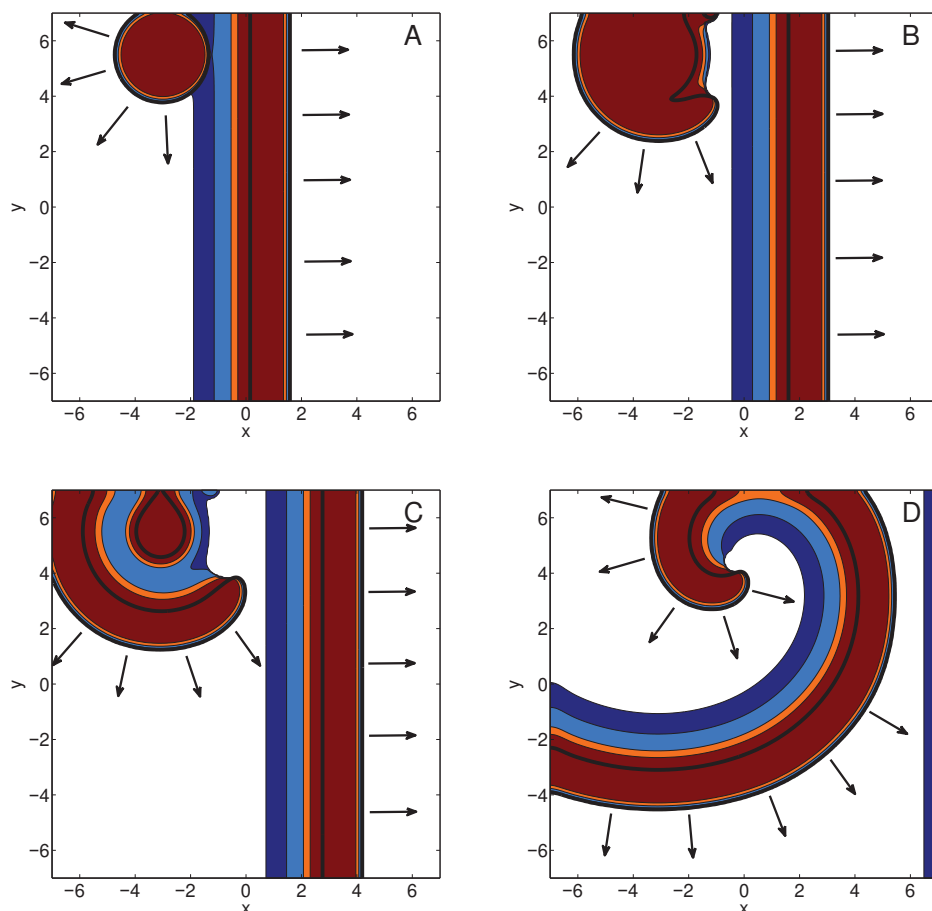


Fig. 3. Generation of a spiral wave due to ectopic activity. See text for details. The black bold line is the contour plot  $u(x, y, t^*) = 0.1$ . The different colored regions represent different levels of refractoriness of the medium. The region in white represents the medium completely recovered and an AP can be elicited. The region in red is a completely unexcitable region as an AP is occurring. The regions in orange and clear blue have a very low excitability level. The region in dark blue is more excitable and an AP might propagate in this region. The arrows point the direction of wave propagation. ( $x$  and  $y$  are in  $cm$ )

A particular and simple way in which the formation of a spiral wave can be explained, is shown in Fig. 3, where a solution of Eq. (2) is shown for four different integration times. In Fig. 3A, a pulse travels from left to right as shown by the direction of the arrows. After the pulse has passed, an ectopic firing appears at the back of the pulse. The ectopic firing starts propagating in all directions except at the back of the front where the region is still in refractory state (Fig. 3B). The abnormal firing generates a curved front with a free end that propagate downwards (Fig. 3C). The original AP moves to the right, disappears at the right boundary and the region that was initially in refractory state is now ready to accept

another AP. Then, the free end can propagate on the recovered region generating a spiral wave (Fig. 3D). After a spiral wave has been generated, if its rotation frequency is faster than the stimulation frequency from the sinoatrial node, then the spiral wave becomes the new pacemaker of the heart (Lee, 1997).

#### 4.1 Meandering and drift of a spiral wave

When a spiral wave evolves in excitable media in general, its dynamics are ruled by (i) the local conducting mechanisms, and; (ii) the heterogeneities of the medium. The former gives rise to a phenomenon called meandering, whereas the later to a phenomenon referred to as drift of a spiral wave.

One way to get a better understanding of meandering and drift of a spiral wave, is by studying the evolution of the position of its tip. The tip of a spiral wave can be defined in a variety of ways and a resume can be found in (Fenton et al., 2002). In this work it is considered the tip of the spiral wave as the point over the level curve  $u = 0.5$  with zero normal velocity (Fenton et al., 2002).

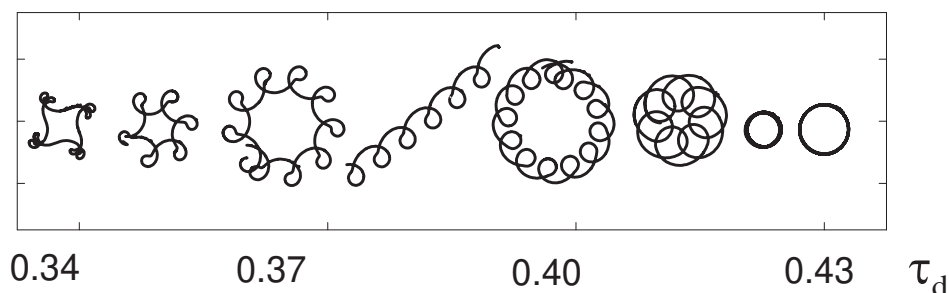


Fig. 4. Tip trajectories of the spiral waves obtained with Eqns. (2), with  $u_c = 0.13$  and varying the parameter  $\tau_d$  from 0.34 to 0.43. An increase in the value  $\tau_d$  implies a reduction in the excitability of the medium.

##### 4.1.1 Meandering of a spiral wave

In Fig. 4, different tip trajectories of spiral waves corresponding to different values of  $\tau_d$  are shown. The value  $\tau_d$  controls the speed at which the depolarizing ions enter to the cell and is a measure of the excitability of the cell (Efimov et al., 1995; Fenton et al., 2002). An increase in the value  $\tau_d$  implies a reduction in the excitability of the medium. When  $\tau_d = 0.43$  the tip of the spiral wave traces a circumference. When the value of  $\tau_d$  is reduced to 0.425 the radius of the circular trajectory is reduced. However, when the value of  $\tau_d$  is reduced to about 0.415 the trajectory is no longer circular but a curve that resembles an epitrochoid (Fig. 5B). Decreasing the value of  $\tau_d$  increases the radius  $R$  (Fig. 5B) of the epitrochoidal trajectory. For  $\tau_d = 0.3965$  the value of  $R$  tends to infinity obtaining a trochoidal trajectory (Epitrochoid with  $R = \infty$ ). For smaller values of  $\tau_d$  the tip trajectory resembles an hypotrochoid of radius  $R$  (Fig. 5A). For values less than  $\tau_d = 0.34$  deformations of hypotrochoidal trajectories are obtained (Fig. 4).

The phenomenon shown in Fig. 4, is called meandering of the tip trajectory or meandering. In order to understand the mechanisms behind meandering it is necessary to study the recovery regions when the spiral wave is propagating in the medium. In Fig. 6, it is shown the contour of the variable  $u(x, y, t^*) = 0.1$  for a particular time  $t^*$  (Labeled bold line in Fig. 6B); Also, are shown different regions corresponding to the level of recovery of the medium, given by the variable  $v$  in Eqns. 2, plotted also for the time  $t^*$ . The region in black means that the region is

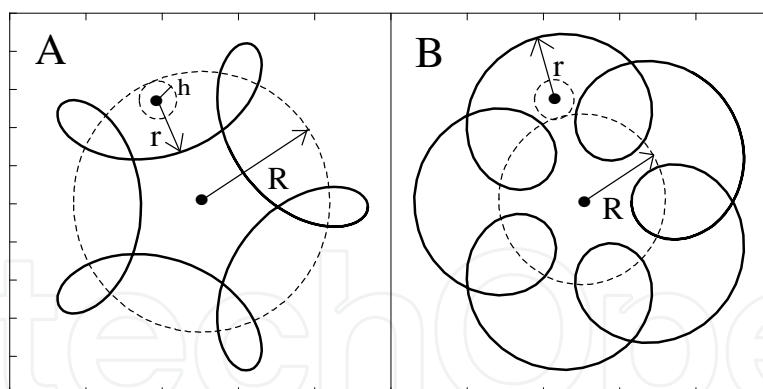


Fig. 5. (A) An hypotrochoid and; (B) an epitrochoid. From (Olmos, 2007)

completely unexcitable ( $v$  in this case is close to zero); As the region becomes clearer, the value of  $v$  gets closer to 1 and therefore the region is able to accept more easily another AP. The line in blue is the trajectory followed by the tip for a time interval around  $t^*$ .

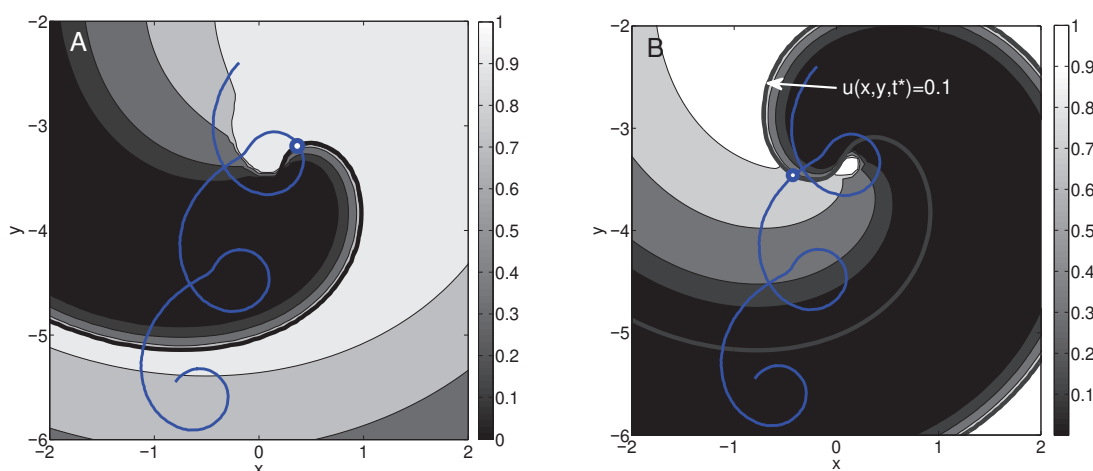


Fig. 6. Propagation of a spiral wave generated with Eqns. (2) with  $\tau_d = 0.3965$ . The line in blue represents the trajectory of the tip. The different coloured regions represents different levels of refractoriness given by the  $v$  variable. For  $v$  close to 0 (black), the region is in its maximum level of refractoriness and an AP cannot be elicited here. For  $v \approx 1$  (white), the region is almost or totally recovered and an AP can be elicited in this region. (A) Formation of a petal; (B) Formation of an arc. The blue dot filled in white, is the location of the tip of the spiral.

In Figures 4 and 6, it is shown that the trajectory of the tip of the spiral wave has high and low curvature in an alternate and periodic fashion. The part with high curvature is referred to as a petal, whereas the part with low curvature, an arc. In Fig. 6A, the tip is tracing a petal, whereas in Fig. 6B, an arc.

In Fig. 6A, it is shown the spiral wave at the time where the tip is tracing a petal. In this case, the front that is close to the tip (blue dot filled in white) of the wave, propagates through a region that is almost completely recovered giving a maximum in the curvature of the trajectory. A different scenario occurs in Fig. 6B, where the tip is tracing an arc. Here, it is clear that the front close to the tip of the spiral propagates through a region that is not

completely recovered. This causes the front to propagate in another direction, where the medium is more excitable. This deviation generates the low curvature part of the trajectory or the arc. This process occurs periodically and the trajectory shown in Fig. 6 is obtained.

In order to give an explanation about the occurrence of the different trajectories obtained in Fig. 4, we use the information of the previous paragraph and the facts that (i)  $1/\tau_d$  is the speed at which the  $Na$  ions enter to the cell to depolarize it. For shorter  $\tau_d$  the ions enter faster to the cell, and; (ii) from Eqns. (2), changing the value of  $\tau_d$  does not affect the threshold value  $u_{th}$ . Consider the case shown in Fig. 6, where  $\tau_d = 0.3965$ , ie, when the tip trajectory is trochoidal. In Fig. 6A, a petal is being traced. When the value of  $\tau_d$  is reduced then the flux of  $Na$  ions (In Eqns. (2),  $I_{fi}$  is carried by  $Na$  ions) is increased. Therefore, the larger amount per time unit of ions with a constant diffusion coefficient, makes that the spiral wave will trace a petal with larger curvature than in the case with  $\tau_d = 0.3965$ . In the same way, it will follow that the front of the spiral wave will reach its own tail before than the case with  $\tau_d = 0.3965$ . Therefore, it is obtained an hypotrochoidal trajectory like the one shown in Fig. 4 with  $\tau_d = 0.37$ . A similar argument follows for epitrochoidal trajectories.

#### 4.1.2 Drift of a spiral wave

Drift of a spiral wave is a directed change of its location with time in response to perturbations (Biktashev, 2007). There are different ways in which drift might occur and an complete list can be found in (Biktashev, 2007). In this work we focus on two different ways in which drift occurs (Fig. 7). In Fig. 7A, it is shown the drift of a spiral wave due to the presence of inhomogeneities. Initially, we considered a spiral wave with  $\tau_d = 0.43$ . With this choice of  $\tau_d$ , the tip of the spiral wave traces a circumference. After some integration time, we changed the value of  $\tau_d$  to 0.39 for  $y < 0$ . The result of this change in the value of  $\tau_d$  is shown in Fig. 7A. In the figure, it is observed that the tip trajectory no longer traces a circumference but a trajectory that resembles a spring. When the tip is far from the interphase  $y = 0$ , the trajectory traces the usual circumference. However, when the tip hits the region above  $y = 0$ , the curvature generated is higher than the curvature below  $y = 0$  due to the decrease in  $\tau_d$ . This causes a drift of the position of the center of the circumference. It follows that the trajectory moves along the line  $y = 0$  where there is a difference in  $\tau_d$  between the two phases.

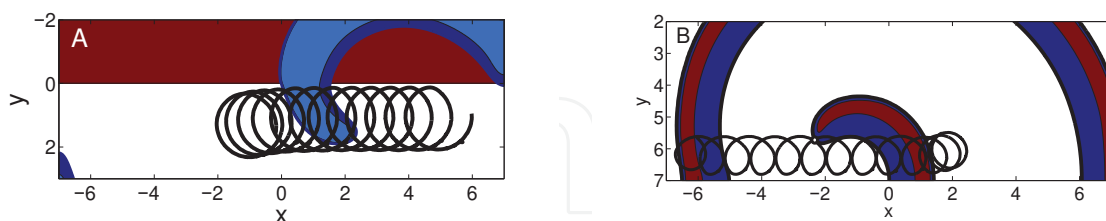


Fig. 7. Drift of a spiral wave due to (A) Inhomogeneities in the medium, and; (B) Interaction with a boundary. In (A)  $\tau_d = 0.43$  for  $y \geq 0$  and  $\tau_d = 0.39$  for  $y < 0$ .

In Fig. 7B, it is shown the drift of a spiral wave due to the presence of a boundary. In this case, when a spiral wave with a circular tip trajectory gets close enough to a boundary, there is an increase in the curvature of the trajectory giving as a consequence drift of the center of the circular trajectory. Therefore, the trajectory drifts along the boundary. The physical mechanism by which the gain in curvature of the trajectory is observed, is apparently as follows: The impermeable boundary prevents the spread of the current produced by the spreading wavefront, which is equivalent to local rise in the excitability of the medium close

to the boundary (Yermakova & Pertsov, 1986), and therefore an increase in the curvature of the trajectory (Subsection 4.1.1).

## 5. Partially excitable obstacles

Partially excitable obstacles are inhomogeneities in the tissue that originate from changes in single-cell properties such as the conductance of ion channels (Shajahan et al., 2009). Such inhomogeneities can arise from damaged or scar tissue (Starobin et al., 1996), when a lesion is created via ablation (Azene et al., 2001) or by regional hyperkalemia (Xie et al., 2001). These changes affect the propagation speed of the pulse (Kléber & Rudy, 2004), the action potential duration (Beeler & Reuter, 1977; Efimov et al., 1995; Shajahan et al., 2009) and prolongs recovery of excitability after the occurrence of an action potential (Xie et al., 2001).

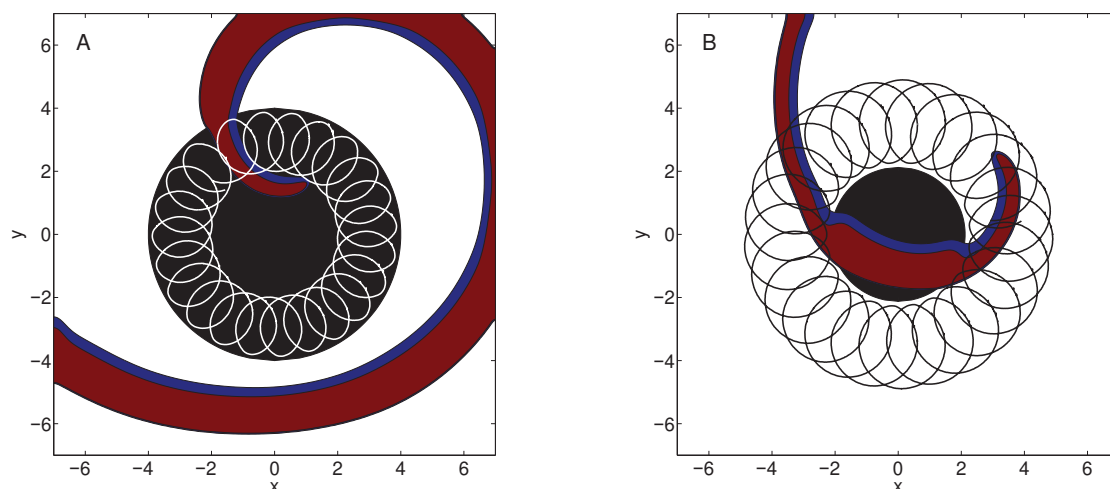


Fig. 8. Tip trajectories of spiral waves obtained with Equations (2) with a partially excitable circular obstacle (A)  $\tau_d = 0.38$  outside the circular obstacle and  $\tau_d = 0.43$  inside,  $r = 4$ ; (B)  $\tau_d = 0.43$  outside the obstacle and  $\tau_d = 0.38$  inside,  $r = \sqrt{4.5}$ .

The stability of spiral waves depending on inhomogeneities in the medium has been studied by Shajahan (Shajahan et al., 2009) and Xie (Xie et al., 2001). In this work, we focus on partially excitable obstacles of circular shape. A pair of simulations are shown in Fig. 8. In Figure 8A,  $\tau_d = 0.38$  outside the circular obstacle and  $\tau_d = 0.43$  inside. The radius of the obstacle is  $r = 4$ . In the previous section, the tip of the spiral wave followed the boundary between the two regions. In Figure 8A, it is shown that the trajectory also follows such boundary, which corresponds to the boundary of the inhomogeneity. In this case, it is shown that the tip traces a curve that resembles an hypotrochoid. In the case where the value of  $\tau_d$  is inverted, i.e.  $\tau_d = 0.43$  outside the inhomogeneity and  $\tau_d = 0.38$  inside, with a radius  $r = \sqrt{4.5}$ , we obtain the trajectory shown in Fig. 8B. Here, the trajectory obtained resembles an epitrochoid. This last result has been presented in (Biktashev, 2007) within a frame of drift due to inhomogeneities where inside the obstacle the refractory period is longer than outside.

Now, consider varying the radius of the obstacle. In Fig. 9 we present the results of considering the two cases presented in Fig. 8. In the top row, we show the case when the trajectory resembles a hypotrochoid. In order to obtain these trajectories, we took  $\tau_d = 0.43$  inside the obstacle, such that inside the obstacle the trajectory is circular. Outside the obstacle  $\tau_d$  was taken as 0.38, such that the trajectory outside is hypotrochoidal. The radius of the

obstacle is increased from left to right. When the radius of the obstacle is less than the radius of the circumference traced by the tip trajectory, the trajectory is circular. As the radius of the obstacle is increased, the trajectory changes from circular to hypotrochoidal. Then, by considering an increase in the radius of the obstacle, the circular trajectory experiences a bifurcation as the one periodic rotation changes to a two period rotation. This result was reported by Mikhailov et al. (Mikhailov et al., 1994) where a circular domain with no flux boundary conditions was considered.

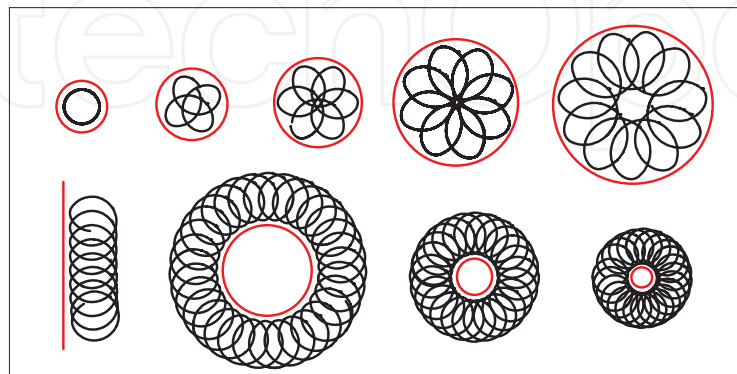


Fig. 9. Trajectories obtained with Eqns. (2) with a partially excitable circular obstacle and different radii. The red circle in each case, represents the boundary of the obstacle. Top row:  $\tau_d = 0.38$  outside the circular obstacle and  $\tau_d = 0.43$  inside. Circular and hypotrochoidal trajectories are obtained; Bottom row  $\tau_d = 0.43$  outside the obstacle and  $\tau_d = 0.38$ . Epitrochoidal trajectories are obtained

In the bottom row of Fig. 9 is shown the case when the trajectory traces an epitrochoid. In this case, if we take a smaller radius, an epitrochoidal trajectory remains even by taking  $R$  tending to zero. Additionally to this result, it is also clear that by considering partially excitable obstacles it is possible to obtain the case of an epitrochoidal trajectory with  $R = \infty$  and therefore a transition between the hypotrochoidal and epitrochoidal cases. Just like the case of meandering discussed in subsection 4.1.1.

The results presented in the top row of Figure 9, have a completely different meaning from those presented in (Mikhailov et al., 1994). As an example, consider the tip trajectory shown in Fig. 10, which corresponds to the upper left case shown in Fig. 9. Initially, the tip of the spiral wave is located outside of the obstacle. Because  $\tau_d = 0.38$  outside the obstacle, an hypotrochoid is obtained. However, as soon as the trajectory hits the obstacle, the tip of the spiral wave gets trapped by the obstacle and the trajectory becomes circular (Fig. 10).

Therefore, in this section we have shown that heterogeneities in the conducting properties of the medium can give different results. (i) If inside the obstacle we take a value of  $\tau_d^1$  such that the tip trajectory is a circumference of radius  $r_1$  and outside the obstacle the value of  $\tau_d$  is less than  $\tau_d^2 < \tau_d^1$ , where  $\tau_d^2$  gives a circular trajectory with radius  $r_2 < r_1$ , then if the radius of the obstacle is  $r \in [r_2, r_1]$  then a circular tip trajectory due to the interaction between the tip of the spiral wave and the obstacle is obtained. Clearly, this case includes the situation of having an epitrochoidal or hypotrochoidal trajectory outside the obstacle (with the values of  $\tau_d$  given in Fig. 4). (ii) Under the same conditions as above but the radius  $r$  of the obstacle larger than  $r_1$ , then the trapped trajectory will trace a hypotrochoid. Observe that in this regime, we can obtain a transition from epitrochoidal (given by meandering) to hypotrochoidal trajectory

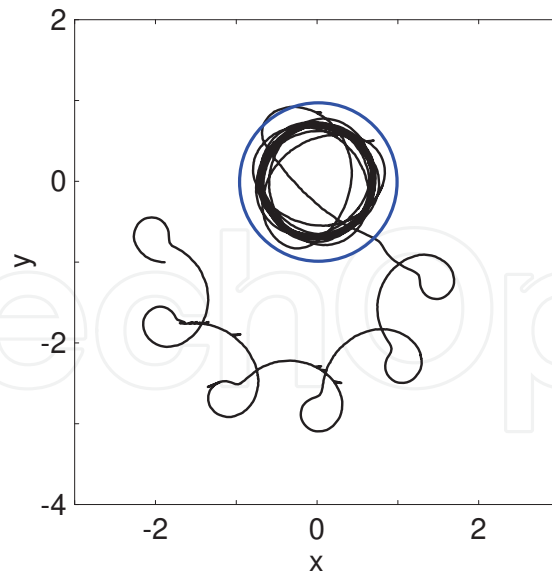


Fig. 10.  $\tau_d = 0.38$  outside  $\tau_d = 0.43$  inside the obstacle. The radius of the obstacle is  $r = 1$ . The simulation was done in the domain  $\Omega = [-7,7] \times [-7,7]$ , but a zoom of the region of interest is shown.  $x$  and  $y$  in cm.

(given by drift of the spiral wave). (iii) Finally, when the values of  $\tau_d$  inside and outside the obstacle are reverted, what is obtained is an epitrochoidal trajectory.

It is important to observe that two periodic rotations, named epitrochoidal and hypotrochoidal trajectories, and transitions from circular to hypotrochoidal regimes, are also obtained through drift. Therefore, the presence of partially excitable obstacles in cardiac tissue may induce the existence of trajectories that mimic the meandering behavior.

## 6. Non-excitable obstacles

Obstacles in cardiac tissue have been modeled with regions where the zero flux condition is imposed (Azene et al., 2001; Isomura et al., 2008; Panfilov & Kenner, 1993; Shajahan et al., 2009; Starobin et al., 1996; Valderrábano et al., 2000). Arteries (Valderrábano et al., 2000) and the natural orifices in the atria, (Azene et al., 2001) are examples of this type of obstacles. Also, these obstacles can be artificially generated in experimental preparations by making cuts in the tissue (Cabo et al., 1996; Ikeda et al., 1997).

The interaction of spiral waves with non excitable obstacles has been considered by different authors (Azene et al., 2001; Ikeda et al., 1997; Isomura et al., 2008; Panfilov & Kenner, 1993; Shajahan et al., 2009; Starobin et al., 1996; Valderrábano et al., 2000). Of particular interest is the work by Ikeda (Ikeda et al., 1997), where it is observed that when a spiral wave attaches to an obstacle, a transition between two different classes of arrhythmias is observed.

In the present section we extend the results observed by Ikeda (Ikeda et al., 1997) and show that the presence of non excitable obstacles, just as the partially excitable ones, can stabilize or destabilize spiral wave dynamics. Initially, it is considered a spiral wave in the circular regime ( $\tau_d = 0.426$ ), with a circular obstacle with radius  $r = 1.7$  and center in the origin. In this regime, we placed the tip of the spiral wave near the obstacle. The result is shown in Fig. 11. In this situation, it is observed that the spiral rotates and at the same time starts moving around the obstacle. Due to the drift at an impermeable boundary plus the circular shape of the obstacle, it is observed that the tip of the spiral traces a curve very similar to an

epitrochoid. Therefore, the presence of a circular obstacle, has changed the simple rotation of the spiral wave into a two periodic rotation. This phenomenon, was observed for obstacles of all sizes above mesh partition. The speed of the drift was a decreasing function of the radius.

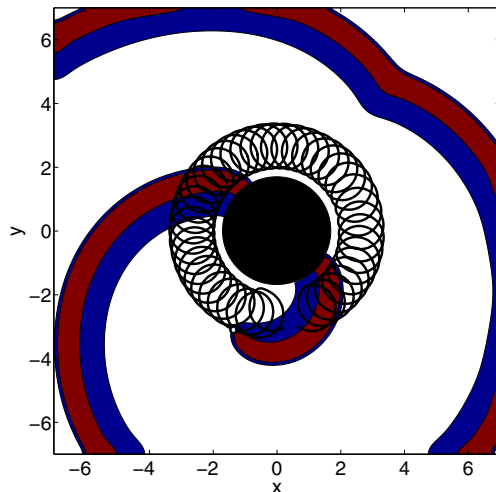


Fig. 11. Drift of a spiral wave around a circular obstacle.  $\tau_d = 0.426$ , radius  $r = 1.7$ .

In our second experiment, we considered a spiral wave in the epitrochoidal regime ( $\tau_d = 0.405$ ). In the same way, we placed the spiral wave in such way that the tip of the spiral interacts with the obstacle. The results are shown in Fig. 12. In the figure, it is shown a spiral wave in the epitrochoidal regime interacting with the circular obstacle at different integration times. In Figs. 12A,B, it is shown that the spiral wave traces an epitrochoid. As soon as the spiral wave hits the boundary, the tip trajectory changes its direction due to the boundary effects (Olmos & Shizgal, 2008; Yermakova & Pertsov, 1986). In the figure, it is shown that the tip of the spiral wave hits the boundary four times. In the first three interactions, it is observed that the spiral bounces at the obstacle. However, in the fourth interaction it is observed that the spiral wave attaches to the obstacle (Fig. 12C). A major consequence obtained is that the two frequency rotation given by the epitrochoidal regime, changes after a transient, to a simple rotation given by the circular regime.

The change from the two rotation period to simple rotation was due to attachment of the spiral wave to the obstacle (Olmos, 2010). However, this experiment raises different questions. When the tip of the spiral hits the obstacle, why in some cases bouncing is observed and then attachment?, Does attachment always occur? Does attachment depend on the size of the radius of the obstacle?, How long it takes to a spiral to attach to the obstacle? To answer these questions is a very difficult task.

In order to show the complexity of this problem, we consider a previous analysis done in (Olmos & Shizgal, 2008). We interact the tip of spiral waves in the trochoidal regime ( $R = \infty$  in Fig.5) with a flat boundary. With these settings we remove the effect of the curvature of the obstacle and the curvature of the epitrochoidal and hypotrochoidal regimes. We took initial conditions such that the trajectory had an incident angle  $\theta_i$  with respect to the boundary (Fig. 13A).

When the tip of a spiral wave interacts with a boundary, there are two possible outcomes. The tip of the spiral wave bounces at the boundary as in Fig. 13A, or disappears at the boundary, in which case the spiral wave also disappears from the domain (Olmos & Shizgal, 2008). When

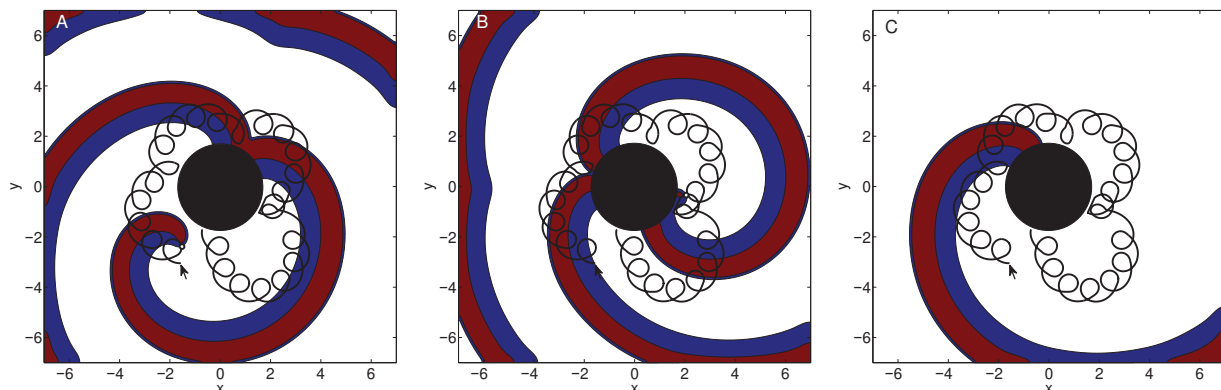


Fig. 12. Interaction of a spiral wave in the epistrochoidal regime with a circular obstacle for different integration times. The arrow points at the place where the trajectory starts. (A) shows the trajectory of the spiral wave meandering; (B) the spiral wave hits the obstacle and bounces, and; (C) the spiral wave hits the obstacle and gets anchored. Note the difference in the frequency of excitation between (A)-(B) and (C).

considering obstacles, the effect of bouncing is the same for a boundary and for the obstacle. However, the effect of annihilation at a boundary becomes attachment of the spiral wave to the obstacle (Olmos, 2010). In Fig. 13B, we show the probability of annihilation of a spiral wave at the boundary as a function of the incident angle, following the procedure in (Olmos & Shizgal, 2008). From the figure, it is clear that for  $\theta_i \in [0^\circ, 60^\circ] \cup [160^\circ, 180^\circ]$  the tip of the spiral wave bounces at the boundary. For  $\theta_i \in (60^\circ, 160^\circ)$  in some cases, there was observed bouncing but also annihilation. As we increase the value of  $\theta_i$  from  $60^\circ$  to  $140^\circ$ , there is an increase in the proportion of spiral waves that annihilate at the boundary. For  $\theta_i = 140^\circ$  all the trajectories considered in the simulations disappeared at the boundary giving annihilation. From there, as the value of  $\theta_i$  is increased up to  $\theta_i = 160^\circ$ , the proportion of spirals that bounced at the boundary increased again.

Based on the previous information, we run several examples in the epistrochoidal regime ( $\tau_d = 0.405$ ) as the one shown in Fig. 12. We considered obstacles with three different radius,  $r = 0.8$ ,  $r = 1.1$  and  $r = 1.7$ . From there, we took all the cases where attachment of the spiral wave to the obstacle was obtained. It was observed from this numerical experiment that the angles at which attachment occurred, ranged from  $10^\circ$  to  $100^\circ$ . From this observation and from Fig. 13B, it is shown that for incident angles  $\theta_i \in [10^\circ, 60^\circ]$ , annihilation at the flat boundary is not possible, but attachment to the circular obstacle is possible.

The phenomenon of obtaining attachment for angles  $\theta_i$  that in the flat boundary gave bouncing might be expected from the studies in (Leal-Soto, 2011; Olmos, 2010), where a spiral wave in the trochoidal regime interacted with the face of a square shaped obstacle. In these studies, it is shown that a spiral wave that would experience bouncing in a flat boundary, will experience attachment to the obstacle, as the interaction of the spiral wave takes place near a corner of the obstacle. Therefore, when we consider a circular obstacle, the interactions of the tip of the spiral wave with the obstacle can be thought as the interaction of the tip of a spiral with a smoothed corner of a square shaped obstacle. This explains why attachment is observed for angles less than  $\theta_i = 60^\circ$  observed in the simulations.

Attachment to the circular obstacle was observed to happen with angles  $\theta_i$  between  $10^\circ$  to  $100^\circ$ . This does not imply that attachment is not possible for  $\theta_i$  outside this range of values. In fact, from the simulations, the interaction of the spiral wave with the obstacle rarely

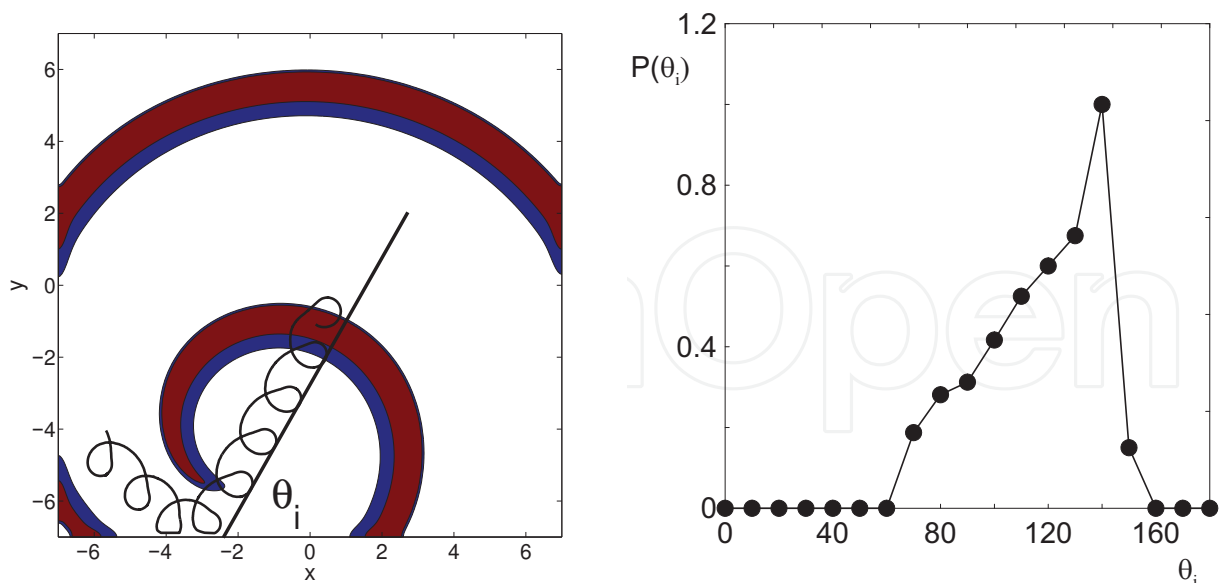


Fig. 13. (A) Interaction of a spiral wave in the trochoidal regime ( $R = \infty$  in Fig. 5,  $\tau_d = 0.3965$ ) with a boundary.  $\theta_i$  is the angle of incidence. In the figure, the tip of the spiral wave bounces at the boundary. (B) Probability of annihilation of the spiral wave at the boundary for a particular angle of incidence  $\theta_i$ .

occurs with angles greater than  $100^\circ$ . This basically happens because we are considering epitrochoidal trajectories. If we consider hypotrochoidal trajectories, then interactions will take place mostly with angles above  $90^\circ$ .

### 6.1 More complex dynamics

The interaction of a meandering spiral wave with an obstacle has different outcomes. In Fig. 14A, we show how complex dynamics can be. We took a spiral wave in the epitrochoidal regime such that the tip touches the obstacle and bounces at it. The dynamics of the tip trajectory are shown in Fig. 14A. From the figure it is clear that the trajectory hits the obstacle repeatedly following no visible pattern. As seen in the figure, there is no attachment of the spiral to the obstacle for large time integrations. Clearly, the activation of the tissue is completely irregular and might be considered as being in a fibrillatory regime.

When we consider an obstacle of a very small size, and an epitrochoidal trajectory, it is observed that the trajectory follows a more stable pattern (Fig. 14B). In this case, the trajectory gets close to the obstacle periodically and it can be said that it happens each time the trajectory traces an epitrochoid. As soon as the tip of the trajectory gets close to the obstacle, the boundary effects induce an increase in the curvature of the trajectory, producing drift of the spiral wave. It is important to note that the increase in the curvature is very small as the size of the obstacle is also very small. This small perturbation in the tip trajectory allows the trajectory to preserve the epitrochoidal trajectory as opposed in what is shown in Fig. 14A.

In this section, we have shown that obstacles might act as a switch between the one and two periodic rotations. Therefore, it follows that the presence of obstacles does not necessarily induce a more stable regime in the spiral wave. Moreover, if the spiral wave is in the epitrochoidal regime, the result might be (i) A transition to a simple rotation scheme; (ii)

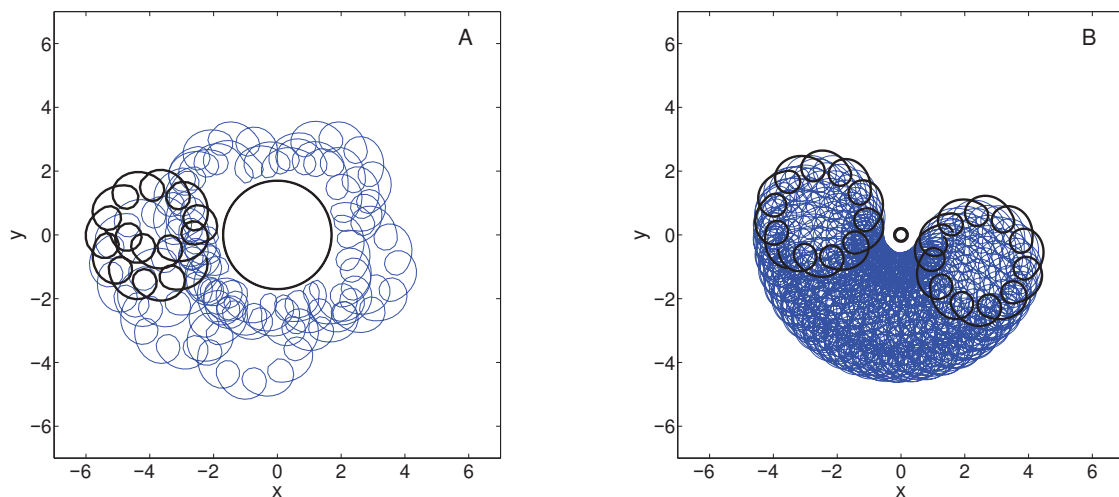


Fig. 14. Tip trajectories traced by a spiral wave solutions of Eqns. (2) when a circular obstacle is imposed. (A) The trajectory does not follow a regular pattern; (B) When the size of the obstacle is small enough a three periodic trajectory is obtained.

A transition to a more complex pattern, and; (iii) if the radius of the obstacle is sufficiently small, a transition to a three period rotation<sup>1</sup>.

## 7. Conclusions, limitations and open questions

In this work, it was considered the interaction of spiral waves in the circular and meandering regime with partially and non excitable obstacles of circular shape. The aim was to understand the transitions that occur between three different regimes: the circular, the epitrochoidal and the hypotrochoidal. The presence of a spiral wave in the circular regime, provides a periodic stimulation of the tissue in a more stable fashion than the other two regimes, as only one excitation frequency is present. When a spiral wave attaches to an obstacle the arrhythmic regime is the same as is the tip of a spiral wave were tracing a circle.

When partially excitable obstacles were considered (Section 5), it was shown that the presence of such inhomogeneities induced the appearance of epitrochoidal and hypotrochoidal trajectories, commonly associated to meandering. This implies that epitrochoidal and hypotrochoidal trajectories might arise due to meandering or drift. It is important to point out that tip trajectories obtained with meandering, like linear trajectories (Fenton et al., 2002), were not obtained with drift. Nonetheless it is important to understand the nature of these trajectories to apply the proper procedure to remove them.

Transitions between different spiral wave regimes were obtained when an obstacle was placed in the medium (Sections 5 and 6). In Section 5, tip trajectories changed from epitrochoidal or hypotrochoidal to circular ones. Also, the reversed process might be obtained, i.e. circular trajectories can switch to epitrochoidal or hypotrochoidal trajectories. Finally, transitions from epitrochoidal to hypotrochoidal might also be obtained. On the other hand, in Section 6, it was shown that the presence of an obstacle, might act as a switch between two different arrhythmic regimes. (i) Simple rotating spirals changed to a two period meandering spiral wave; (ii) Two periodic meandering spiral waves changed to (a) simple rotating spiral; (b) Three periodic meandering spiral wave and; (c) More complex trajectory with no regular pattern associated.

<sup>1</sup> Strictly speaking, the trajectory is not three periodic, but there are three frequencies associated to the tip motion.

In general, it was shown that the presence of inhomogeneities in the medium not only stabilizes the spiral wave dynamics as shown in (Ikeda et al., 1997; Kim et al., 1999; Shajahan et al., 2007) but also might generate more complex dynamics, which implies that the presence of obstacles might induce a more dangerous arrhythmic regime than the one without the obstacle.

Drift of a spiral wave had been considered only for planar boundaries (Yermakova & Pertsov, 1986) and inside circular domains (Mikhailov et al., 1994). In this work, it was presented the drift of a spiral wave around a circular obstacle which was not previously reported. Up to now, there are still missing conditions for general shape obstacles that allow drift of the spiral wave around the obstacle, when the spiral tip traces a circle. A similar analysis for partially excitable obstacles is missing. i.e. which geometric properties must have an obstacle such that the tip trajectory of a spiral wave will follow its boundary?

The study of attachment of meandering spiral waves to non-excitable obstacles is a very difficult task, as there is not a clear a pattern that relates the radius of the obstacle and the radius of the epitrochoid. Also, it is still the question of studying which type of trajectory, epitrochoidal or hypotrochoidal, will attach more easily to an obstacle of a given size. In this work it was not considered the study of hypotrochoidal trajectories and non-excitable obstacles as the original study was to establish conditions to consider an obstacle as a switch between the circular and epitrochoidal regime.

## 8. Acknowledgements

The author would like to acknowledge ACARUS at the University of Sonora, for their facilities for the numerical computations. This work was supported by PROMEP.

## 9. References

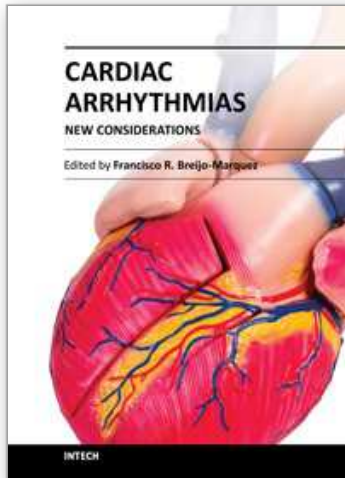
- Azene, E. M.; Trayanova, N. A. & Warman, E. (2001). Wave Front-obstacle interactions in cardiac tissue: a computational study. *Ann. Biomed. Eng.*, Vol. 29, No. 1, (January 2001) (35-46), 0090-6964
- Beeler, G. W. & Reuter, H. (1977). Reconstruction of the action potential of ventricular myocardial fibres. *J. Physiol.*, Vol. 268, No. 1, (June 1977) (177-210) 0022-3751
- Benson, A. P. & Holden, A. V. (2005). Calcium oscillations and ectopic beats in virtual ventricular myocytes and tissues: bifurcations, autorhythmicity and propagation, In: *Lecture Notes in Computer Science*, Frangi, F; Radeva P. I.; Santos A. & Hernandez, Springer, (895-897), Springer-Verlag Berlin, 3-540-26161-3, Berlin, Germany
- Biktashev V. N. (2007). Drift of spiral waves. *Scholarpedia*, Vol. 2, No. 4, (2007) (1836), 1941-6016
- Cabo, C.; Pertsov, A. M.; Davidenko, J. M.; Baxter, W. T.; Gray, R. A. & Jalife J. (1996). Vortex shedding as a precursor of turbulent electrical activity in cardiac muscle. *Biophys. J.*, Vol 70, No. 3, (March 1996) (1105-1111), 0006-3495
- Comtois, P. & Vinet, A. (2005). Multistability of reentrant rhythms in an ionic model of a two-dimensional annulus of cardiac tissue. *Phys. Rev. E*, Vol. 72, No. 5, (November 2005) 051927(1-11), 1539-3755
- Courtemanche, M.; Ramirez, R. J. & Nattel S. (1998). Ionic mechanisms underlying human atrial action potential properties: insights from a mathematical model. *Am. J. Physiol. and Heart Circ. Physiol.*, Vol. 275, No. 1, (July 1998) (H301-H321), 0363-6135

- Davidenko, J. M.; Pertsov, A. V.; Salomonsz, R.; Baxter, W. & Jalife, J. (1992). Stationary and drifting spiral waves of excitation in isolated cardiac muscle. *Nature*, Vol. 355, No. 6358, (January 1992) (349-351), 0028-0836
- DiFrancesco, D. & Noble, D. (1985). A model of cardiac electrical activity incorporating ionic pumps and concentration changes. *Phil. Trans. R. Soc. Lond.*, Vol. 307, No. 1133, (January 1985), (353-398), 0962-8436
- Efimov, I. R.; Krinsky, V. I.; & Jalife, J. (1995). Dynamics of rotating vortices in the Beeler-Reuter model of cardiac tissue. *Chaos, Sol. and Frac.*, Vol. 5, No.3-4 (March-April 1995) (513-526), 0960-0779
- Fenton, F. H. & Cherry, E. M. (2008). Models of cardiac cell. *Scholarpedia*, Vol. 3, No. 8, (2008) (1858), 1941-6016
- Fenton, F. H. & Karma, A. (1998). Vortex dynamics in three-dimensional continuous myocardium with fiber rotation: Filament instability and fibrillation. *CHAOS*, Vol. 8, No. 1, (March 1998) (20-47), 1054-1500
- Fenton, F. H.; Cherry, E.; Hastings, H. M. & Evans, S. J. (2002). Multiple mechanisms of spiral wave breakup in a model of cardiac electrical activity. *CHAOS*, Vol. 12, No. 3, (September 2002) (852-892), 1054-1500
- Hodgkin, A. L. & Huxley, A. F. (1952). A quantitative description of membrane current and its application to conduction and excitation in nerve. *J. Physiol*, Vol. 117, (August 1952), (500-544), 0022-3751
- Ikeda, T.; Yashima, M.; Uchida, T.; Hough, D.; Fishbein, M. C.; Mandel, W. J.; Chen, P. S. Karagueuzian, H. (1997). Attachment of meandering reentrant wave fronts to anatomic obstacles in the atrium - Role of the obstacle size. *Circ. Res.*, Vol. 81, No. 5, (November 1997) (753-764), 0009-7330
- Isomura, A.; Hörning, M.; Agladze, K. & Yoshikawa, K. (2008). Eliminating spiral waves pinned to an anatomical obstacle in cardiac myocytes by high-frequency stimuli. *Phys. Rev. E*. Vol. 78, No. 6, (December 2008) 066216(1-6), 1539-3755
- Kim, Y.; Xie, F.; Yashima, M.; Wu, T.; Valderrábano, M.; Lee, M.; Ohara, T.; Voroshilovsky, O.; Doshi, R. N.; Fishbein, M. C.; Qu, Z.; Garfinkel, A.; Weiss, J. N.; Karagueuzian, H. S. & Chen, P. (1999). Role of papillary muscle in the generation and maintenance of reentry during ventricular tachycardia and fibrillation in isolated swine right ventricle. *Circulation*, Vol. 100, No. 13, (September 1999), 1450-1459, 0009-7322
- Kléber, A. G. & Rudy, Y. (2004). Basic Mechanisms of cardiac impulse propagation and associated arrhythmias. *Physiol. Rev.*, Vol. 84, No. 2, (April 2004) (431-488), 0031-9333
- Leal-Soto, D. A. (2011). M. Sc. Thesis: Interacción de ondas en espiral y obstáculos en medios excitables con la ecuación de Fitzhugh-Nagumo (In Spanish). Universidad de Sonora, México.
- Lee K.J. (1997) Wave Pattern Selection in an Excitable System. *Phys. Rev. Lett.* Vol. 79, No. 15, (October 1997) (2907-2910) 0031-9007
- Lim, Z. Y.; Maskara, B.; Aguel, F.; Emokpae R. & Tung, L. (2006). Spiral wave attachment to millimeter-sized obstacles. *Circulation*, Vol 114, No. 20 (November 2006) (2113-2121), 0009-7322
- Luo, C.-S. & Rudy, Y. (1994). A Dynamic Model of the Cardiac Ventricular Action Potential.I. Simulations of ionic currents and concentration changes. *Circ. Res.*, Vol. 74, No. 8, (June 1994) (1071-1096), 0009-7330

- Luo, C.-S. & Rudy, Y. (1994). A Dynamic Model of the Cardiac Ventricular Action Potential.II. Afterdepolarizations, triggered activity, and potentiation. *Circ. Res.*, Vol. 74, No. 8, (June 1994) (1097-1113), 0009-7330
- Mikhailov, A. S.; Davydov, V. A.; Zykov, V. S. (1994). Complex dynamics of spiral waves and motion of curves. *Physica D*, Vol 70, No. 1-2, (January 1994) (pages 1-39) 0167-2789
- Morton K. W. & Mayers D. F. (2005). *Numerical Solution of Partial Differential Equations*, Cambridge University Press, 978-0-521-60793-0, Cambridge.
- Nygren, A.; Fiset, C; Firek, L.; Clark, J. W.; Lindblad, D.S.; Clark, R. B.; Giles W. R. (1998). Mathematical Model of an Adult Human Atrial Cell: The Role of  $K^+$  Currents in Repolarization *Circ. Res.*, Vol 82, No. 1, (January 1998) (63-81), 0009-7330
- Olmos, D. (2007). Ph. D. Thesis: Pseudospectral solutions of reaction-diffusion equations that model excitable media: convergence of solutions and Applications. University of British Columbia, Canada.
- Olmos, D. & Shizgal B. D. (2008). Annihilation and reflection of spiral waves at a boundary for the Beeler-Reuter model. *Phys. Rev. E*, Vol. 77, No. 3, (March 2008) (031918 1-14), 1539-3755
- Olmos, D. (2010). Reflection and attachment of spirals at obstacles for the Fitzhugh-Nagumo and Beeler-Reuter models. *Phys. Rev. E*, Vol. 81, No. 4, (April 2010) 041924(1-9), 1539-3755
- Otani, N. F. (2000). Mini Review: Computer Modeling in Cardiac Electrophysiology. *J. Comput. Phys.*, Vol. 161, No. 1, (June 2000) (21-34), 0021-9991
- Panfilov, A. V. & Keener, J. P. (1993). Effects of high frequency stimulation on cardiac tissue with an inexcitable obstacle, *J. Theor. Biol*, Vol. 163, No. 4, (August 1993) (439-448), 0022-5193
- Pertsov, A. M.; Davidenko, J. M.; Salomonsz, R.; Baxter, W. T. & Jalife, J. (1993). Spiral waves of excitation underlie reentrant activity in isolated cardiac muscle. *Circ. Res.*, Vol. 72, No. 3, (March 1993) 631-650, 0009-7330
- Priebe, L. & Beuckelmann, D. J. (1998). Simulation Study of Cellular Electric Properties in Heart Failure. *Circ. Res.*, Vol. 82, No. 11 (June 1998) (1206-1223) 0009-7330
- Priori, S. G.; Aliot, E.; Blømsstrom-Lundqvist, C.; Bossaert, L.; Breithardt, G.; Brugada, P.; Camm, J. A.; Cappato, R.; Cobbe, S. M.; Di Mario, C.; Maron, B. J.; McKenna, W. J.; Pedersen, A. K.; Ravens U.; Schwartz, P. J.; Trusz-Gluza, M.; Vardas, P.; Wellens, H. J. J. & Zipes, D. P. (2002). Task Force on Sudden Cardiac Death, European Society of Cardiology. *Europace*, Vol. 4 (January 2002) (3-18), 1099-5129
- Shajahan, T. K.; Sinha, S. & Pandit, R. (2007). Spiral-wave dynamics depend sensitively on inhomogeneities in mathematical models of ventricular tissue. *Phys. Rev. E*, Vol. 75, No. 1, (January 2007) 011929(1-8), 1539-3755
- Shajahan, T. K.; Nayak, A. R. & Pandit, R. (2009) Spiral-Wave Turbulence and its Control in the Presence of Inhomogeneities in Four Mathematical Models of Cardiac Tissue. *Plos One*, Vol. 4, No. 3, (March 2009) (1-21), 1932-6203
- Starobin, J. F.; Zilberter, Y. I.; Rusnak, E. M. & Starmer, C. F. (1996). Wavelet formation in excitable cardiac tissue: the role of wavefront-obstacle interactions in initiating high-frequency fibrillatory-like arrhythmias. *Biophys. J.*, Vol. 70, No. 2, (February 1996) (581-594), 0006-3495
- Tang, A. S.; Ross, H.; Simpson, C. S.; Mitchell, L. B.; Dorian, P.; Goeree, R.; Hoffmaster, B.; Arnold M. & Talajic, M. (2005). Canadian cardiovascular society / Canadian

- heart rhythm society position paper on implantable cardioverter defibrillator use in Canada. *Can J. Cardiol*, Vol. 21, Suppl A, (May 2005) (11A-18A), 0828-282X
- Ten Tusscher, K. H. W. J. & Panfilov, A. V. (2002). Reentry in heterogeneous cardiac tissue described by the Luo-Rudy ventricular action potential model. *Am J. Physiol. Heart Circ. Physiol.*, Vol. 284, No. 2, (February 2002) (H542-H548), 0363-6135
- Valderrábano, M.; Kim, Y.-H.; Yashima, M.; Wu, T.-J.; Karagueuzian, H. S. & Chen, P.-S. (2000). Obstacle-induced transition from ventricular fibrillation to tachycardia in isolated swine right ventricles: Insights into the transition dynamics and implications for the critical mass. *J. Am. Col. Cardiol.*, Vol. 36, No. 6, (November 2000) (2000-2008), 0735-1097
- Veenhuizen, G. D.; Simpson, C. S. & Abdollah, H. (2004). Atrial Fibrillation. *CMAJ*, Vol. 171, No. 7, (September 2004) (755-760), 0820-3946
- Xie, F.; Qu, Z.; Garfinkel A. & Weiss J. N. (2001). Effects of simulated ischemia on spiral wave stability. *Am. J. Heart Circ. Physiol.*, Vol. 280, No. 4, (April 2001) (H1667-H1673). 0363-6135
- Yanagihara, K.; Noma, A. & Irisawa, H. (1980). Reconstruction of sino-atrial node pacemaker potential based on the voltage clamp experiments. *Jap. J. Physiology*, Vol. 30, No. 6, (1980) (841-857), 0021-521X
- Yermakova, Y. A. & Pertsov, A. M. (1986). Interaction of rotating spiral waves with a boundary. *Biophysics*, Vol. 31, No. 5, (932-940) 0006-3509
- Zaret, B. L.; Moser, M. & Cohen, L. S. (1992). *Yale University School of Medicine Heart Book*, Hearst books, 0-688-09719-7, New York.
- Zipes, D. P. (2005). Epidemiology and mechanisms of sudden cardiac death. *Can J. Cardiol*, Vol. 21, Suppl A, (May 2005) (37A-40A), 0828-282X

IntechOpen



## **Cardiac Arrhythmias - New Considerations**

Edited by Prof. Francisco R. Breijo-Marquez

ISBN 978-953-51-0126-0

Hard cover, 534 pages

**Publisher** InTech

**Published online** 29, February, 2012

**Published in print edition** February, 2012

The most intimate mechanisms of cardiac arrhythmias are still quite unknown to scientists. Genetic studies on ionic alterations, the electrocardiographic features of cardiac rhythm and an arsenal of diagnostic tests have done more in the last five years than in all the history of cardiology. Similarly, therapy to prevent or cure such diseases is growing rapidly day by day. In this book the reader will be able to see with brighter light some of these intimate mechanisms of production, as well as cutting-edge therapies to date. Genetic studies, electrophysiological and electrocardiographic features, ion channel alterations, heart diseases still unknown, and even the relationship between the psychic sphere and the heart have been exposed in this book. It deserves to be read!

### **How to reference**

In order to correctly reference this scholarly work, feel free to copy and paste the following:

Daniel Olmos-Liceaga (2012). Spiral Waves, Obstacles and Cardiac Arrhythmias, Cardiac Arrhythmias - New Considerations, Prof. Francisco R. Breijo-Marquez (Ed.), ISBN: 978-953-51-0126-0, InTech, Available from: <http://www.intechopen.com/books/cardiac-arrhythmias-new-considerations/spiral-waves-obstacles-and-cardiac-arrhythmias->

**INTECH**  
open science | open minds

### **InTech Europe**

University Campus STeP Ri  
Slavka Krautzeka 83/A  
51000 Rijeka, Croatia  
Phone: +385 (51) 770 447  
Fax: +385 (51) 686 166  
[www.intechopen.com](http://www.intechopen.com)

### **InTech China**

Unit 405, Office Block, Hotel Equatorial Shanghai  
No.65, Yan An Road (West), Shanghai, 200040, China  
中国上海市延安西路65号上海国际贵都大饭店办公楼405单元  
Phone: +86-21-62489820  
Fax: +86-21-62489821

© 2012 The Author(s). Licensee IntechOpen. This is an open access article distributed under the terms of the [Creative Commons Attribution 3.0 License](#), which permits unrestricted use, distribution, and reproduction in any medium, provided the original work is properly cited.

IntechOpen

IntechOpen